Pressure dependence of dynamical heterogeneity in water

2008 J. Phys.: Condens. Matter 20 244116

(http://iopscience.iop.org/0953-8984/20/24/244116)

J. Phys.: Condens. Matter **20** (2008) 244116 (7pp) doi:10.1088/0953-8984/20/24/244116

Pressure dependence of dynamical heterogeneity in water

Victor Teboul

Laboratoire des Propriétés Optiques des Matériaux et Applications, CNRS UMR 6136, Université d'Angers, 2 Boulevard Lavoisier, F-49045 Angers, France

E-mail: victor.teboul@univ-angers.fr

Received 4 March 2008
Published 29 May 2008
Online at stacks.iop.org/JPhysCM/20/244116

Abstract

Using molecular dynamics simulations we investigate the effect of pressure on the dynamical heterogeneity in water. We show that the effect of a pressure variation in water is qualitatively different from the effect of a temperature variation on the dynamical heterogeneity in the liquid. We observe a strong decrease of the aggregation of molecules of low mobility together with a decrease of the characteristic time associated with this aggregation. However, the aggregation of the most mobile molecules and the characteristic time of this aggregation are only slightly affected. In accordance with this result, the non-Gaussian parameter shows an important decrease with pressure while the characteristic time t^* of the non-Gaussian parameter is only slightly affected. These results highlight then the importance of pressure variation investigations in low temperature liquids on approach to the glass transition.

1. Introduction

The existence of cooperative molecular motion in supercooled glass-forming liquids is commonly invoked [1] as the likely explanation for the dramatic increase of the viscosity as the liquid is cooled toward its glass transition. Cooperative motions associated with heterogeneous dynamics are also commonly postulated in order to explain the non-exponential behavior of correlation functions and the non-Arrhenius behavior [2] with temperature of the viscosity of most glass-forming liquids. Dynamical heterogeneities and associated cooperative behavior have been reported either experimentally near the glass transition temperature or with molecular dynamics simulations well above this temperature [2, 3]. From MD simulations these heterogeneities are usually characterized by an aggregation of the most mobile molecules and of the least mobile molecules [2–16]. Because the structure changes only slightly when the temperature of the liquid decreases, the increase of the cooperative motions predicted by most theories has been associated with the observed dynamical heterogeneities. Whether dynamical heterogeneities are partly at the origin of the strange comportment of glass-forming liquids or are only an interesting consequence of it is, however, still a matter of conjecture.

The microscopic dynamical and structural behavior of water is of fundamental interest due to its many unique properties compared to other liquids [17]. The pressure dependence of the viscosity and diffusion coefficient of this liquid displays for example a well known counterintuitive behavior. While the temperature dependence of the dynamical heterogeneity has been studied in a number of articles only few works have been done on its pressure evolution. It seems then of particular interest to investigate the evolution of dynamical heterogeneity with pressure inside supercooled water in order to shed some light on the link between these heterogeneities and the structural and dynamical behavior of supercooled water. In this paper we investigate with molecular dynamics simulations the pressure dependence of dynamical heterogeneity in supercooled water. We show that the effect of pressure is qualitatively different from the effect arising from a temperature variation, showing that pressure is an important complementary parameter for the study of cooperative motions in supercooled liquids.

2. Calculation

The present simulations were carried out for a system of 506 water molecules (506O + 1012H). Our simulations use the Gear algorithm with the quaternion method [18] to solve the equations of motion with the TIP5PE potential [19–21]. This potential is an improvement of the TIP5P potential [20, 21], which was reported to be one of the most realistic potentials in

Table 1. Characteristic times and maximum values of $I^{+/-}(t)$ and $\alpha_2(t)$ in bulk water at a temperature of 250 K for various pressures. Characteristic times $t^{+/-}$ and t^* are defined as the times corresponding to the maximum of the functions $I^{+/-}(t)$ and $\alpha_2(t)$.

Pressure (MPa)	Part of the pressure due to molecular interactions (MPa)	$\alpha_2(t^*)$	$I^+(t^+)$	$I^-(t^-)$	D (10^{-5} cm^2 s^{-1})	$D^*\tau_\alpha$ (Å^2)	τ_α (ps)	Characteristic time t^* (ps)	Characteristic time t^+ (ps)	Characteristic time t^- (ps)
58.3	−55.3	0.95	28	22.8	0.283	0.368	13	6	4	58
149.2	29.9	0.62	24	17.4	0.50	0.325	6.5	4	3	20
288.5	161.4	0.38	18	13	0.75	0.30	4	2.1	2	7
520.5	384.0	0.32	20.5	12.2	0.75	0.30	4	2.0	2	5.7

water. The time step was chosen equal to 10^{-15} s. The reaction field method [18] was employed to take into account long-range electrostatic interactions with a cutoff radius of 9 Å. The simulations are aged for 20 ns in order to insure stabilization before any treatment. In order to avoid fluctuations in the box size, the density was set constant in our simulations, at 0.982, 1.03, 1.10 and 1.18 g cm^{-3}. The temperature was fixed in our simulations at 250 K using a Berendsen thermostat [22]. The pressures were then calculated inside the simulation using the formula

$$P = \rho k_B T + \frac{1}{3V}\left\langle \sum_{i<j} \mathbf{F_{ij}} \cdot \mathbf{r_{ij}} \right\rangle. \quad (1)$$

The mean calculated pressures corresponding to the four different densities were, respectively, $P = 58.3$, 149.2, 288.5 and 520.5 MPa.

In the Markovian approximation, the self-part of the Van Hove correlation function $G_s(r, t)$ has a Gaussian form. This function is defined by

$$G_s(\mathbf{r}, t) = \left\langle \frac{1}{N} \sum_{i=1}^{N} \delta(\mathbf{r} + \mathbf{r}_i(t_0) - \mathbf{r}_i(t + t_0)) \right\rangle \quad (2)$$

and $4\pi r^2 G_s(r, t)$ represents the probability for a particle to be at time $t + t_0$ at a distance r from its position at time t_0. Departure from this Gaussian form has been found in various glass-forming liquids and is thought to be due to dynamical heterogeneities. Such deviations are usually characterized by the non-Gaussian parameter

$$\alpha_2(t) = \frac{3\langle r^4(t)\rangle}{5\langle r^2(t)\rangle^2} - 1 \quad (3)$$

where $\langle r^2(t)\rangle$ is the mean square displacement.

Another interesting quantity to investigate is the intermediate incoherent scattering function (IISF). This function describes the autocorrelation of the density fluctuations at the wavevector Q:

$$F_S(Q, t) = \frac{1}{N} \mathrm{Re}\left(\sum_i \mathrm{e}^{\mathrm{i}\mathbf{Q}\cdot(\mathbf{r}_i(t) - \mathbf{r}_i(0))} \right). \quad (4)$$

We define the mobility $\mu_{i,t0}(t)$ of molecule i at time t_0 within a characteristic time t, by the relation

$$\mu_{i,t0}(t) = |\mathbf{r}_i(t + t_0) - \mathbf{r}_i(t_0)|/(\langle r^2(t)\rangle)^{0.5}. \quad (5)$$

The mobility of molecule i at time t_0 is then defined as the normalized displacement of molecule i during a time t. We will omit in further discussion the time t_0, which will disappear in the mean statistical values. We then select molecules of high or low mobility for the calculation of dynamical heterogeneity. This selection is then dependent on the time t chosen for the definition of the mobility $\mu_i(t)$. We define here as most mobile (MM) the 6 per cent of molecules with highest mobility, and as least mobile (LM) the 6 per cent of molecules with lowest mobility. We then select molecules of high and low mobility for the calculation of dynamical heterogeneity. This selection of molecules of high and low mobility depends on the time t chosen in the definition of the mobility. We define here the function

$$A^+(r, t) = g_{\mathrm{mm}}(r)/g(r) - 1. \quad (6)$$

In this formula $g_{\mathrm{mm}}(r)$ is the radial distribution function between centers of mass of the most mobile water molecules, and $g(r)$ is the mean radial distribution function between two molecules. $A(r, t)$ gives a measure of the correlation increase between mobile molecules. Similarly, we define $A^-(r, t)$ for the least mobile molecules.

We then define the integrals $I^{+/-}(t)$ of the functions $A^{+/-}(r, t)$ by

$$I^{+/-}(t) = \int_0^{R_C} A^{+/-}(r, t) 4\pi r^2 \, \mathrm{d}r. \quad (7)$$

In order to eliminate noise effects on the evolution of the function $I(t)$, we have truncated the integral in the following calculations at a cutoff value $R_C = 6$ Å. In our notations, functions $A^-(r, t)$ and $I^-(r, t)$ correspond to the least mobile molecules while functions $A^+(r, t)$ and $I^+(t)$ correspond to the most mobile molecules. Functions $A(r, t)$ represent the correlation increase between molecules of approximately the same mobility, and with distance of r. Functions $I(t)$ represent then the global increase of the correlation between molecules of high (I^+) or low (I^-) mobility. Following [16] we will name the function $I(t)$: intensity of the aggregation.

3. Results and discussion

The diffusion coefficients calculated for the different pressures investigated are listed in table 1. The anomalous increase in D is qualitatively reproduced by our simulations, but the quantitative increase of D is significantly larger than that observed experimentally. As in SPCIE model simulations [23] the maximum of the diffusion coefficient versus pressure is shifted to a higher pressure than in real water [24]. NMR experiments have observed a maximum of diffusion at a

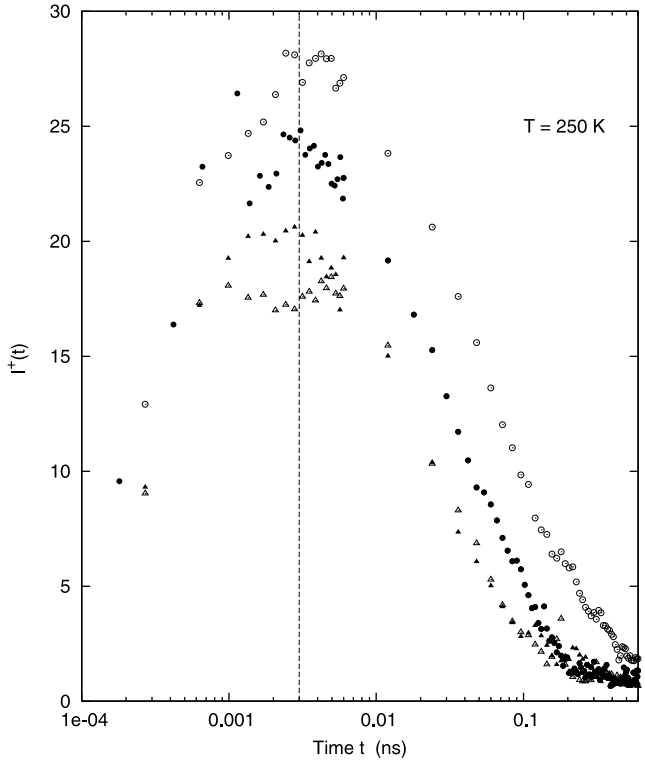

Figure 1. Function $I^+(t) = \int_0^{R_c} A^+(r,t)4\pi r^2\,\mathrm{d}r$ with $R_c = 6$ Å, for the centers of mass of the water molecules. Different pressures are considered: empty circles, $P = 58.3$ MPa; full circles, $P = 149.2$ MPa; empty triangles, $P = 288.5$ MPa; full triangles, $P = 520.5$ MPa. The temperature is 250 K.

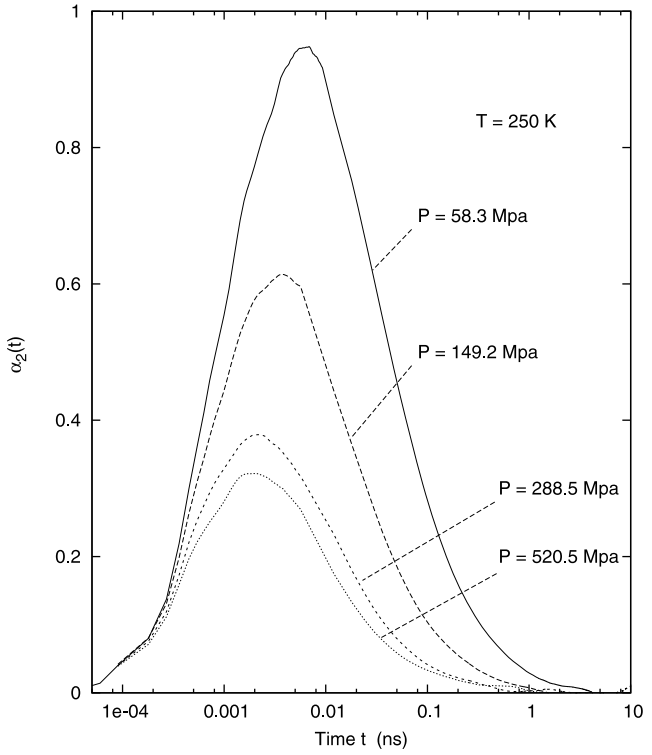

Figure 2. Non-Gaussian parameter of the centers of mass in supercooled water for various pressures. The temperature is 250 K. From bottom to top: continuous line, $P = 58.3$ MPa; short dashed line, $P = 149.2$ MPa; bold dashed line, $P = 288.5$ MPa; dotted line, $P = 520.5$ MPa.

pressure of 150 MPa for $T = 250$ K. For a pressure of 150 MPa the simulation match the experimental data [24] for D ($D_{\mathrm{exp}} = 0.51 \times 10^{-5}$ cm^2 s^{-1} and $D_{\mathrm{calc}} = 0.50 \times 10^{-5}$ cm^2 s^{-1}). While for the other pressures investigated a difference of 30%–60% is found [24, 25]. The larger differences are observed at the larger pressures investigated here.

Figure 1 shows the intensity $I^+(t)$ (as defined in II) of the aggregation of the most mobile molecules (MMMs) for different pressures ranging from 58.3 to 520.5 MPa in supercooled water at a temperature of 250 K. Figure 1 shows that the aggregation of the most mobile water molecules decreases when the pressure increases from 58.3 to 288.5 MPa. The intensity $I^+(t)$ decreases by a factor of 1.55 when the pressure increases from 58.3 to 288.5 MPa. This trend then reverses and $I^+(t)$ increases by a factor of 1.14 when the pressure increases from 288.5 to 520.5 MPa. We define the characteristic time t^+ as the time corresponding to the maximum of the intensity $I^+(t)$ then of the aggregation between mobile molecules. Figure 1 shows that this characteristic time t^+ evolves relatively slightly with pressure from 4 ps for a pressure of 58.3 MPa to 2 ps at a pressure of 520.5 MPa. Figure 2 shows the non-Gaussian parameter of the centers of mass of the water molecules for various pressures. We observe in figure 2 a decrease of the non-Gaussian parameter when the pressure increases. The NGP is usually associated with the presence of dynamical heterogeneity in a supercooled liquid. It has been shown that the NGP evolution follows the evolution of the dynamical heterogeneity and of the aggregation of the most mobile molecules in various liquids including water [14, 16]. Figure 2 then confirms the decrease of the dynamical heterogeneity with the pressure increase in water. The maximum value of the NGP decreases from 0.95 at a pressure of 58.3 MPa to 0.38 at a pressure of 288.5 MPa, then by a factor of 2.5 in this pressure range. This decrease by a factor of 2.5 is then larger than the decrease by a factor of 1.55 of the intensity of the aggregation of the most mobile molecules. Moreover, we observe that the NGP decreases significantly when the pressure increases from 288.5 to 520.5 MPa, while the intensity $I^+(t)$ increases slightly.

The characteristic time of the NGP, defined as the time t^* corresponding to the maximum value of the NGP, has been found to govern string-like motions and the aggregation of the MMMs in various supercooled liquids [4, 5]. Figure 2 shows that the characteristic time t^* of the NGP varies only slightly with pressure, a result that is in accordance with the slight evolution of the characteristic time of the aggregation of the MM water molecules. Moreover, the comparison of figures 1 and 2 shows that t^* corresponds approximately to the characteristic time of aggregation of the MM molecules for the whole set of pressures investigated. The corresponding values of t^* and t^+ are listed in table 1. However, we see in these figures that the non-Gaussian parameter decreases more rapidly than the intensity of the aggregation of the most mobile molecules when the pressure increases. We then observe with pressure variation, a decrease of the MMM heterogeneity

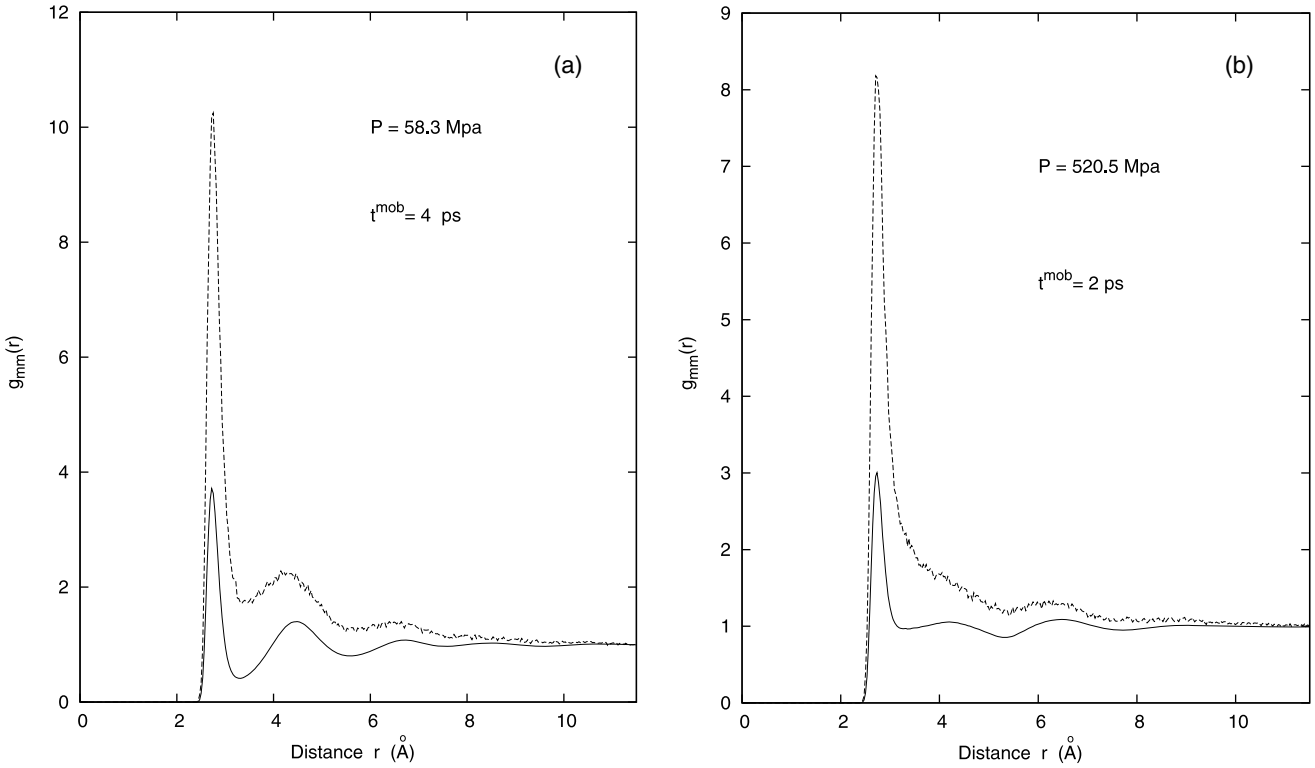

Figure 3. (a) Radial distribution function between centers of mass of the water molecules. Full line, RDF between mean water molecules; dashed line, RDF between the most mobile water molecules. The temperature is 250 K and the pressure $P = 58.3$ MPa. (b) The same as figure 3(a) but at a pressure $P = 520.5$ MPa.

and a decrease of the NGP without the important variation of the characteristic times observed when temperature is the variation parameter. We also observe that the NGP evolves differently with pressure than the intensity of aggregation of the MMMs, in contrast to what is observed when temperature is the variation parameter.

In order to evaluate more precisely the modification of the aggregation of the MMMs when pressure rises, we will now investigate directly the modification of the radial distribution functions between MMM centers of mass. Figures 3(a) and (b) show the radial distribution functions (RDFs) between the MMMs for a pressure of 58.3 MPa (figure 3(a)) and a pressure of 520.5 MPa (figure 3(b)). The times chosen for the mobility selection are here equal to t^+, then the radial distribution functions displayed correspond to the maximum of the aggregation for these pressures. The mean radial distribution functions between centers of mass of the water molecules are displayed for comparison in the same figures. Figures 3(a) and (b) show that the position of the peaks of the RDF for the MMMs corresponds to the positions of the peaks of the mean RDF at the same pressure. The MMMs follow then the structural changes of the bulk liquid when the pressure rises. Figures 3(a) and (b) show that the pressure acts mainly on the first and second peaks of the radial distribution function between MMMs. The decrease of the first peak in the RDF of the MMMs when pressure rises follows the decrease of the first peak of the mean RDF and then roughly does not affect the intensity $I^+(t)$. The main change appears around the second peak (second neighbor). For high pressure in figure 3(b) the RDF oscillation is less pronounced than for low pressure in figure 3(a). Figures 3(a) and (b) show that this structural change decreases the aggregation of the most mobile molecules as the structure of the liquid approaches the structure of the aggregation of the MMMs.

We will now investigate the effect of pressure on the aggregation of the least mobile water molecules (LMMs). Figure 4 shows the intensity $I^-(t)$ (as defined above) of the aggregation of the least mobile water molecules for various pressures at a temperature of 250 K. Figure 4 shows a strong decrease of the aggregation of the LMMs when pressure increases. In contrast to what has been found in figure 1 for the MMMs, figure 4 shows a sharp decrease of the characteristic times of these aggregations when pressure increases. The characteristic time associated with the LMMs decreases from 20 ps at 58.3 MPa to 2 ps at 520.5 MPa, reaching the MMM characteristic time for this pressure. We then observe for high pressures a superposition of the intensity $I^+(t)$ and $I^-(t)$ time evolution, as is only observed for supercooled liquids around the fusion temperature T_f. However, for T around T_f the intensities $I^+(t)$ and $I^-(t)$ merge totally (for times and intensity values), in contrast to what is observed here, where only the time evolution merges due to the different comportment of the two kind of aggregations with pressure. For high pressure the values of the intensities of the aggregations are then higher for the MMMs than for the LMMs.

Figures 5(a) and (b) show the RDF between centers of mass of the least mobile molecules for two different pressures.

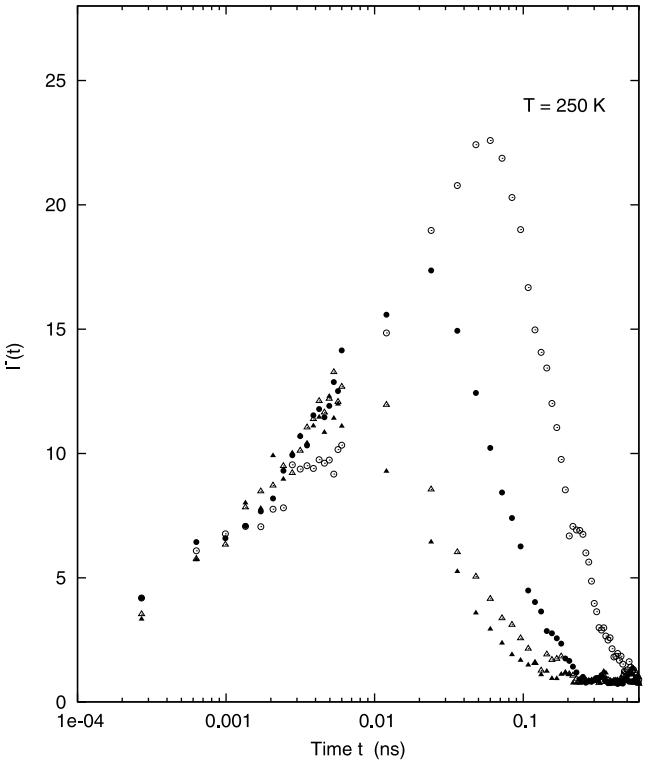

Figure 4. Function $I^-(t) = \int_0^{R_C} A^-(r,t)4\pi r^2\,\mathrm{d}r$ with $R_c = 6$ Å, for the centers of mass of the water molecules. Different pressures are considered: empty circles, $P = 58.3$ MPa; full circles, $P = 149.2$ MPa; empty triangles, $P = 288.5$ MPa; full triangles, $P = 520.5$ MPa. The temperature is 250 K.

The mean radial distribution functions for these pressures are displayed in the same figures for comparison. Figures 5(a) and (b) show that the position of the peaks of the RDF for the LMMs is the same as for the mean molecules. The least mobile molecule aggregation follows then the structural changes of the liquid when the pressure rises. The same result has been observed for the MMMs in figures 3(a) and (b). For the lowest pressure investigated figure 5(a) shows that the LMM aggregates are more ordered than the mean. Actually, the peaks of the RDF of the LMMs are more pronounced and the first minimum is smaller than in the mean RDF. Figure 5(b) shows the same behavior; however, the structural order is much less pronounced at high pressure. The mean RDF shows a decrease of the first and second peaks when pressure rises. Figure 5 shows that the structural order of the liquid decreases sharply when pressure rises. We see in figure 5 that the LMMs follow the same tendency.

Figure 6 shows the mean square displacement $\langle r^2(t)\rangle$ of centers of mass of the water molecules for various pressures at a temperature of 250 K. We observe in figure 6 the three time regimes typical for supercooled liquids. For timescales below 0.3 ps the ballistic time regime, then the plateau and for timescales larger than 10 ps the diffusive time regime. During the ballistic time regime, the temperature (here 250 K) determines the mean square displacement, and we then observe that the different curves superimpose in this regime. Figure 6 shows that for large times (diffusive time regime) the MSD increases with pressure from 58.3 MPa to 288.5 MPa. Then the diffusion coefficient that may be deduced from these curves increases with pressure in this pressure range. However, for

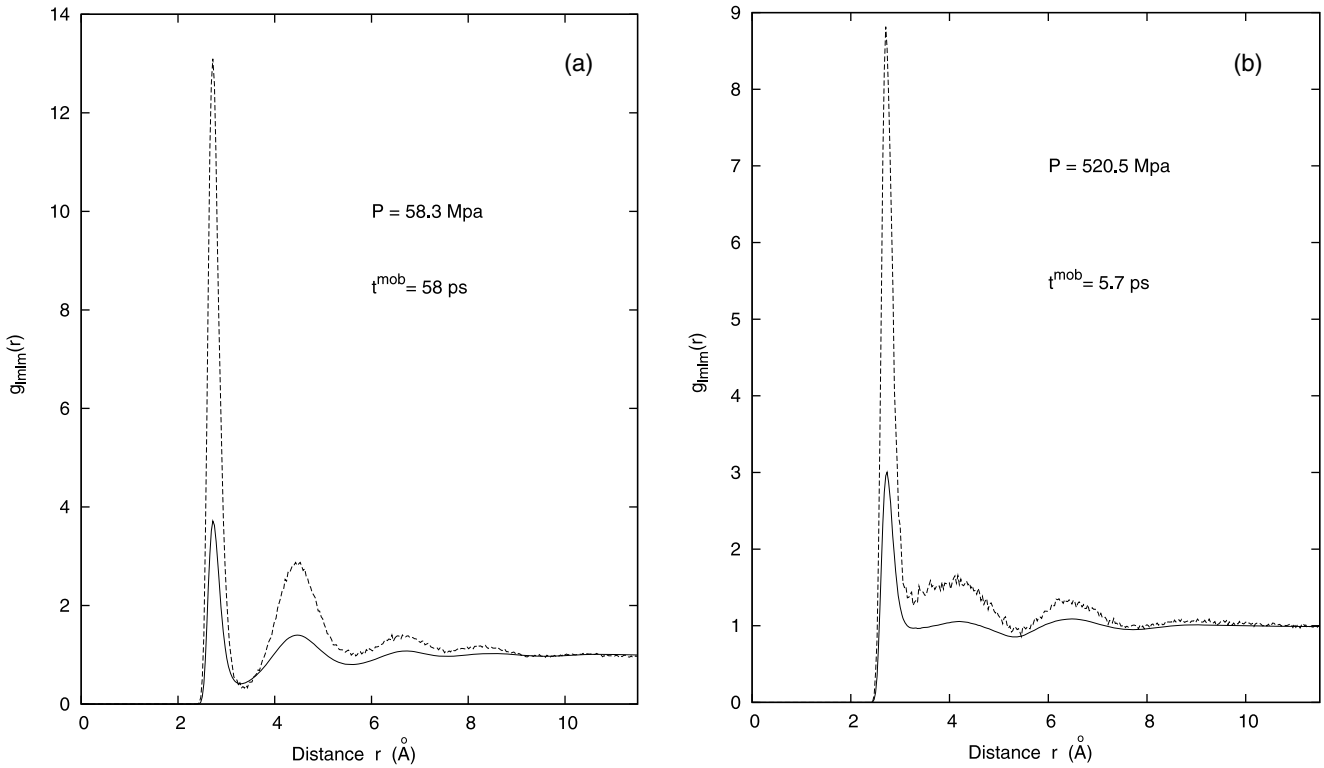

Figure 5. (a) Radial distribution function between centers of mass of the water molecules. Full line, RDF between mean water molecules; dashed line, RDF between the least mobile water molecules. The temperature is 250 K and the pressure $P = 58.3$ MPa. (b) The same as (a) but at a pressure $P = 520.5$ MPa.

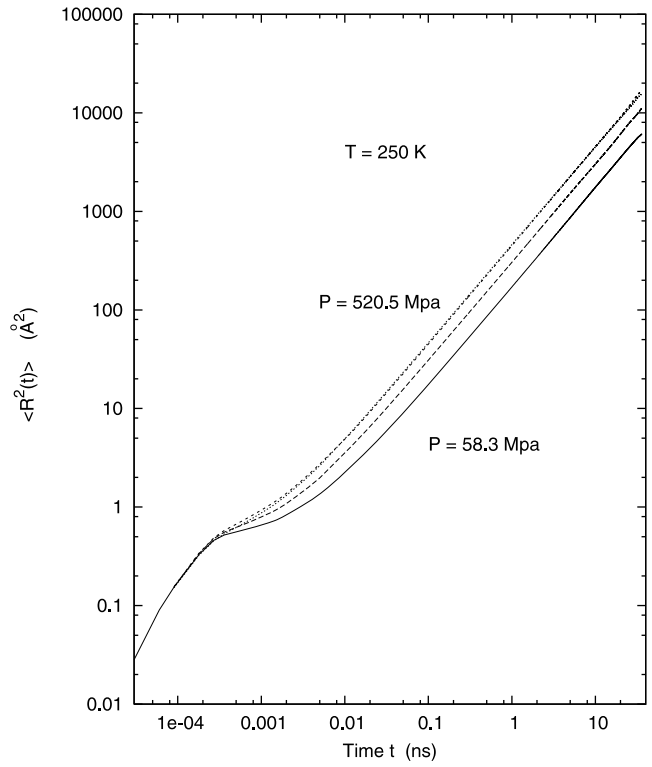

Figure 6. Mean square displacement of the centers of mass of the water molecules ($Å^2$) in supercooled water at various pressures. The temperature is 250 K. From bottom to top: continuous line, $P = 58.3$ MPa; dashed line, $P = 149.2$ MPa; short dashed line, $P = 288.5$ MPa; dotted line, $P = 520.5$ MPa. $\langle r^2(t)\rangle$ is plotted in a logarithmic scale.

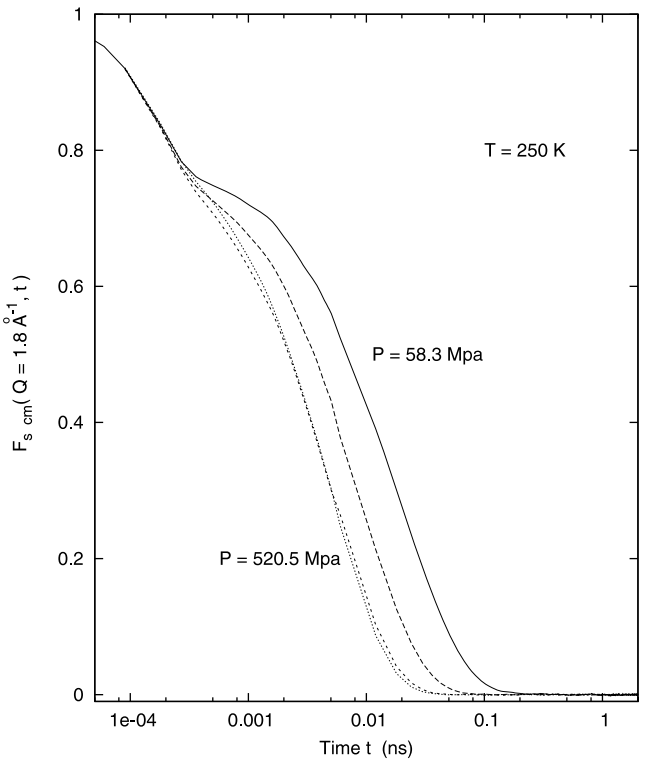

Figure 7. Intermediate incoherent scattering function of the centers of mass of the water molecules for different pressures and at a temperature of 250 K. From top to bottom: continuous line, $P = 58.3$ MPa; dashed line, $P = 149.2$ MPa; short dashed line, $P = 288.5$ MPa; dotted line, $P = 520.5$ MPa.

pressures higher than 288.5 MPa this trend changes and the curves corresponding to 288.5 and 520.5 MPa superimpose on the figure. We observe in figure 6 the same behavior for the plateau timescale. For the two highest pressures displayed the plateau roughly disappears. We also observe in figure 6 that the MSD changes appear at the beginning of the plateau and not at the end of the plateau time regime, as would be expected for an effect governed by cage breaking. The values of the diffusion coefficients deduced from these curves are displayed in table 1.

Figure 7 shows the intermediate incoherent scattering function $Fs(Q, t)$ for centers of mass of the water molecules for various pressures for a wavevector $Q = 1.8$ $Å^{-1}$. $Q = 1.8$ $Å^{-1}$ corresponds here to the maximum of the structure factor at atmospheric pressure. We observe in figure 7 approximately the same behavior as for the MSD in figure 6. The curves corresponding to 288.5 and 520.5 MPa superimpose. The comparison between figures 6 and 7 shows that the evolution of the incoherent scattering function is larger than the evolution of the MSD with pressure. Table 1 shows that the alpha relaxation time decreases by a factor of 3.25 while the diffusion coefficient increases by a factor of 2.65 when pressure rises from 58.3 to 520.5 MPa. From simple theoretical arguments it has been suggested that the mean square displacement and the diffusion mechanism may be associated with the most mobile molecules' behavior, while the intermediate incoherent scattering function and the viscosity may be associated with the least mobile molecules' behavior inside the heterogeneity [2]. From this viewpoint, the larger decrease of the alpha relaxation time than the diffusion characteristic time may be related with the larger decrease of the LMMs than the MMMs when pressure rises.

Figure 8 shows that the radial distribution changes with pressure increase. When the pressure rises, figure 8 shows that the structural order decreases inside the liquid. The structure changes then with pressure. This structural modification, that induces at least partly the modification of the dynamics, shows that the physics behind the pressure effect is qualitatively different from the physics behind the temperature effect on the heterogeneity, because a variation of temperature modifies only slightly the structure of water, in contrast to a variation of pressure. Figure 8 shows that the first peak height decreases when pressure rises, while a simple calculation shows that due to the broadening of the peak the coordination number of the first shell of neighbors increases with pressure. This structural modification on the first shell of neighbors may then affect the aggregation of the least mobile molecules, decreasing their ability to create aggregates and decreasing the lifetime of these aggregates, while for the most mobile molecules the structure effect that may arise from the cage breaking process modification appears to be smaller. Polyamorphism and in particular the presence of a liquid–liquid transition between HDL and LDL water have been discussed in a number of papers [26–31]. The structural difference between LDL and

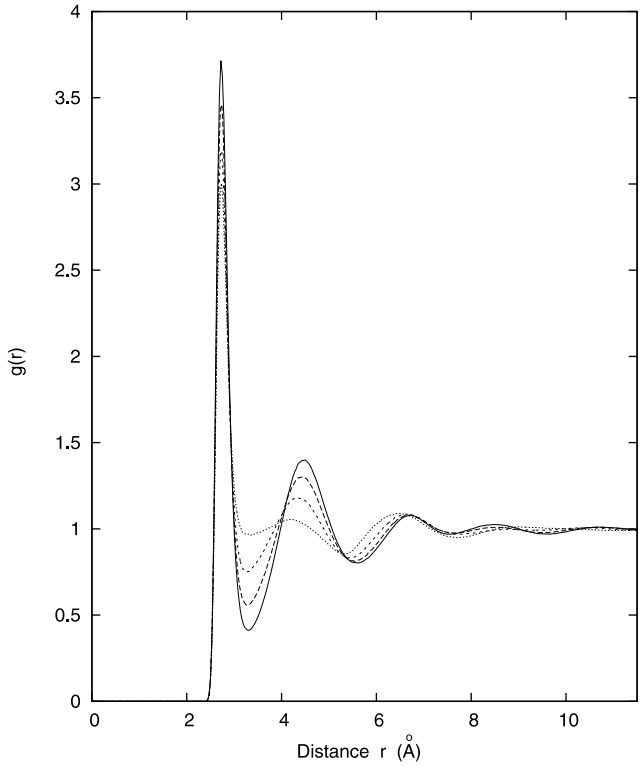

Figure 8. Radial distribution function between centers of mass of the water molecules for various pressures at a temperature of 250 K. Continuous line, $P = 58.3$ MPa; dashed line, $P = 149.2$ MPa; short dashed line, $P = 288.5$ MPa; dotted line, $P = 520.5$ MPa.

HDL is expected to lead to different dynamical behaviors, and then to affect the dynamical heterogeneity as we approach the transition [31]. An anomalous evolution of the dynamical heterogeneity as a function of pressure or temperature may then indicate the presence of the transition. However, the temperature investigated here (250 K) is probably too large to observe this effect. Simulations at lower temperatures and pressures may then give information on the transition and work is in progress to investigate this problem.

4. Conclusion

Using molecular dynamics simulations we have investigated the effect of pressure on the dynamical heterogeneity in supercooled water. We have shown that the effect of a pressure variation in supercooled water is qualitatively different from the effect of a temperature variation on the dynamical heterogeneity in the liquid. We have observed a strong decrease of the aggregation of molecules of low mobility together with a decrease of the characteristic time associated with this aggregation. However, the aggregation of the most mobile molecules and the characteristic time of this aggregation are only slightly affected. The non-Gaussian parameter shows an important decrease with pressure while the characteristic time t^* of the non-Gaussian parameter is only slightly affected. In accordance with these results, the viscosity of the liquid appears to be affected differently than the diffusion coefficient. The important structural changes observed when the pressure rises seems to be at the origin of these evolutions of the dynamical heterogeneity. This result is different from the temperature evolution of the dynamical heterogeneity. These results highlight then the importance of pressure variation investigations in supercooled liquids.

References

[1] Adam G and Gibbs J H 1965 *J. Chem. Phys.* **43** 139
[2] Ediger M D 2000 *Annu. Rev. Phys. Chem.* **51** 99
[3] Sillescu H 1999 *J. Non-Cryst. Solids* **243** 81
[4] Kob W, Donati C, Plimpton S J, Poole P H and Glotzer S C 1997 *Phys. Rev. Lett.* **79** 2827
[5] Donati C, Douglas J F, Kob W, Plimpton S J, Poole P H and Glotzer S C 1998 *Phys. Rev. Lett.* **80** 2338
[6] Yamamoto R and Onuki A 1998 *Phys. Rev. Lett.* **81** 4915
[7] Yamamoto R and Onuki A 1998 *Phys. Rev.* E **58** 3515
[8] Kerrache A, Teboul V, Guichaoua D and Monteil A 2003 *J. Non-Cryst. Solids* **322** 41
[9] Teboul V and Alba-Simionesco C 2005 *Chem. Phys.* **317** 245
[10] Teboul V 2006 *Eur. Phys. J* B **51** 111
[11] Giovambattista N, Buldyrev S V, Starr F W and Stanley H E 2003 *Phys. Rev. Lett.* **90** 085506
[12] Becker S R, Poole P H and Starr F W 2006 *Phys. Rev. Lett.* **97** 055901
[13] Mazza M G, Giovambattista N, Starr F W and Stanley H E 2006 *Phys. Rev. Lett.* **96** 057803
[14] Teboul V, Monteil A, Fai L C, Kerrache A and Maabou S 2004 *Eur. Phys. J.* B **40** 49
[15] Vogel M and Glotzer S C 2004 *Phys. Rev.* E **70** 061504
[16] Teboul V, Maabou S, Fai L C and Monteil A 2005 *Eur. Phys. J.* B **43** 355
[17] Angell C A, Bressel R D, Hemmati M, Sare E J and Tucker J C 2000 *Phys. Chem. Chem. Phys.* **2** 1559
[18] Allen M P and Tildesley D J 1990 *Computer Simulation of Liquids* (New York: Oxford University Press)
[19] Rick S W 2004 *J. Chem. Phys.* **120** 6085
[20] Mahoney M W and Jorgensen W L 2000 *J. Chem. Phys.* **112** 8910
[21] Mahoney M W and Jorgensen W L 2001 *J. Chem. Phys.* **114** 363
[22] Berendsen H J C *et al* 1997 *J. Phys. Chem.* **91** 6269
[23] Starr F W, Sciortino F and Stanley H E 1999 *Phys. Rev.* E **60** 6757
[24] Prielmeier F X, Lang E W, Speedy R J and Ludemann H D 1987 *Phys. Rev. Lett.* **59** 1128
[25] Gillen K T, Douglass D C and Hoch M J R 1972 *J. Chem. Phys.* **57** 5117
[26] McMillan P F, Wilson M, Wilding M C, Daisenberger D, Mezouar M and Neville Greaves G 2007 *J. Phys.: Condens. Matter* **19** 415101
[27] Loerting T and Giovambattista N 2006 *J. Phys.: Condens. Matter* **18** R919
[28] Koza M M, May R P and Schober H 2007 *J. Appl. Crystallogr.* **40** S517
[29] Koza M M, Hansen T, May R P and Schober H 2006 *J. Non-Cryst. Solids* **352** 4988
[30] Nelmes R J, Loveday J S, Strassle T, Bull C L, Guthrie M, Hamel G and Klotz S 2006 *Nature Phys.* **2** 414
[31] Starr F W, Bellissent-Funel M C and Stanley H E 1999 *Phys. Rev.* E **60** 1084